

The Possible Origins of the VR Magnification Ratios of Q0957+561AB

A. Ullán¹, L.J. Goicoechea¹, R. Gil–Merino¹, M. Serra–Ricart², J.A. Muñoz³, E. Mediavilla², J. González–Cadelo¹ and A. Oscoz²

¹Departamento de Física Moderna, Universidad de Cantabria, Avda. de Los Castros s/n, E-39005 Santander, Cantabria, Spain; email: aurora.ullan@postgrado.unican.es, goicol@unican.es, gilmerinor@unican.es, juan.gonzalezc@alumnos.unican.es

²Instituto de Astrofísica de Canarias, C/ Vía Láctea s/n, E-38205 La Laguna, Tenerife, Spain; email: mserra@ot.iac.es, emg@ll.iac.es, aoscoz@ll.iac.es

³Departament d'Astronomia i Astrofísica, Universidad de Valencia, Dr. Moliner 50, E-46100 Burjassot, Spain; email: jmunoz@uv.es

Abstract. We present VR magnification ratios of the double quasar Q0957+561AB, which are inferred from frames taken with the 2.56m Nordic Optical Telescope. From two different photometric techniques (*pho2comC* and *psfphot*) and a reasonable range for the time delay in the system (415–430 days), we find optical continuum ratios depending on the wavelength. These chromatic ratios are consistent with either differential extinction in a dust system or gravitational microlensing in the deflector. Although the dusty scenario is only viable for a compact dust cloud in the line of sight to the A component, the possible values for the differential extinction and the ratio of total to selective extinction in the V band are surprisingly reasonable. To decide on the true origin of the anomalous ratios (extinction, microlensing or a mixed scenario), we are carrying out new monitoring campaigns and planning detailed observations from the best ground-based and space telescopes.

1. Introduction

QSO 0957+561 was the first discovered lensed quasar (Walsh *et al.* 1979) and it is an important laboratory to study the evolution of multiwavelength magnification ratios in a lens system and the nature of the involved physical phenomena. However, although a lot of magnification ratios were measured during the last twenty years, there is no a fair and complete picture accounting for them. The magnification ratio (in magnitudes) is defined as the difference between the magnitude of Q0957+561A and the time delay corrected magnitude of Q0957+561B. At an observed wavelength λ and time t , the ratio is $\Delta m_{AB}(\lambda, t) = m_A(\lambda, t) - m_B(\lambda, t + \Delta t_{AB})$, where Δt_{AB} is the time delay between the two components. Different studies have established that the radio magnification ratio does not depend on the time and it is close to -0.31 mag (e.g., Conner *et al.* 1992). Moreover, the optical emission-lines ratio agrees with the radio magnification ratio: $\Delta m_{AB}(\text{radio}) \approx \Delta m_{AB}(\text{emission-lines}) \approx -0.31$ mag (e.g., Schild & Smith 1991). These ratio/optical results suggest that the macrolens magnification ratio must be of -0.31 mag. In the optical continuum, the situation is more confused, but there is evidence in favour of a R -band ratio in the range 0–0.1.

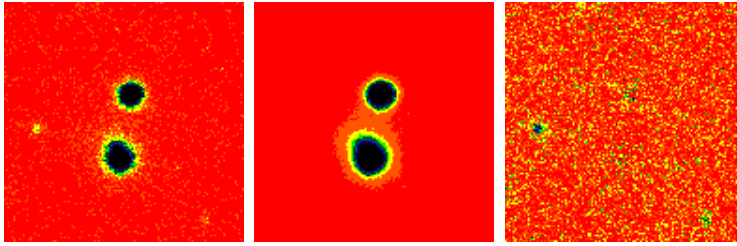


Figure 1. A real frame in the R band (left), the model frame from *psfphot* (centre) and the residual or difference frame (right).

2. Observations and reduction process

We observed QSO 0957+561 from 2000 February 3 to 2000 March 31, as well as two nights in 2001 April. All observations were made with the 2.56m Nordic Optical Telescope (NOT) in the V and R bands. The main period (in 2000) corresponds to the Gravitational Lenses International Time Project (GLITP) monitoring. In 2001 only the frames on April 10 were finally useful for photometric tasks. We used the Bessel V and R passbands, with effective wavelengths of $\lambda_V = 0.536 \mu\text{m}$ and $\lambda_R = 0.645 \mu\text{m}$, respectively. The images are available in the Web site of the Gravitational LENSES and DARK MATTER (GLEN DAMA) project: <http://grupos.unican.es/glendama/>.

We use two different photometric methods in order to get robust results. First of all, we take the Q0957+561A fluxes (Ullán *et al.* 2003) that were derived from the photometric approaches: *pho2com* (Serra–Ricart *et al.* 1999) and *psfphot*. This leads to two datasets consistent each other. Secondly, we use Ullán *et al.* (2003) GLITP correction laws to extract clean fluxes for the *pho2com* results of Q0957+561B on 2001 April 10. The combined (*pho2com* + *corr*) technique is called *pho2comC*. Finally, we also obtain the fluxes of the B component on 2001 April 10 with the *psfphot* task. In this photometric technique, the way to determine the brightnesses of the two quasar components is from PSF fitting (see the example in Figure 1).

3. Optical continuum magnification ratios

From the GLITP brightness records of the A component and the about 14 months delayed Q0957+561B fluxes, one can find the V -band and R -band magnification ratios. The V -band (blue filled circles) and R -band (red filled circles) ratios are presented in Figure 2. While the top panel contains the results from *pho2comC*, the bottom panel includes the *psfphot* results. Given an optical filter, a photometric task and a time delay Δt_{AB} , we compare the B component flux and the corresponding A component fluxes in a 5-days bin. We obtain different V and R magnification ratios. Hence, these ratios are not achromatic, and it is apparent that the higher ratio corresponds to the smaller wavelength. The Oslo group also reported VR fluxes of QSO 0957+561 using the same telescope in the same seasons (see Ovaldsen *et al.* 2003), but through a different photometric technique and a time delay of 416 days. Their typical values $\Delta m_{AB}(\lambda_V) = 0.065 \text{ mag}$ (blue open circles in Fig. 2) and $\Delta m_{AB}(\lambda_R) = 0.026 \text{ mag}$ (red open circles in Fig. 2) agree with our results, so we confirm the absence of strongly biased results. As the VR estimates for a given photometry do not seem to be very sensitive to the delay value, we introduce delay-averaged VR ratios. In a first step, we obtain the effective measurements of the ratios from the averages of the typical values and errors for the different delays. In a second step, taking into account the estimates from the two

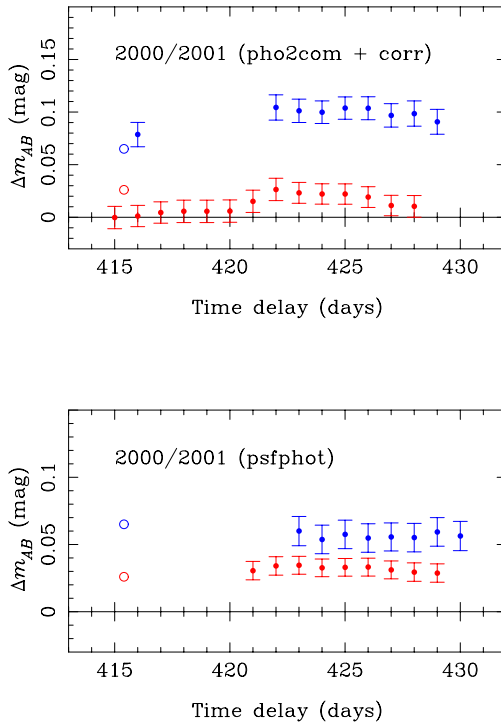


Figure 2. QSO 0957+561 magnification ratios in 2000 (2000/2001 seasons). Blue and red points are associated with ratios in the *V* and *R* bands, respectively. The filled circles are our measurements and the open circles are the typical estimates by the Oslo group (they used a different photometric technique).

EXTINCTION

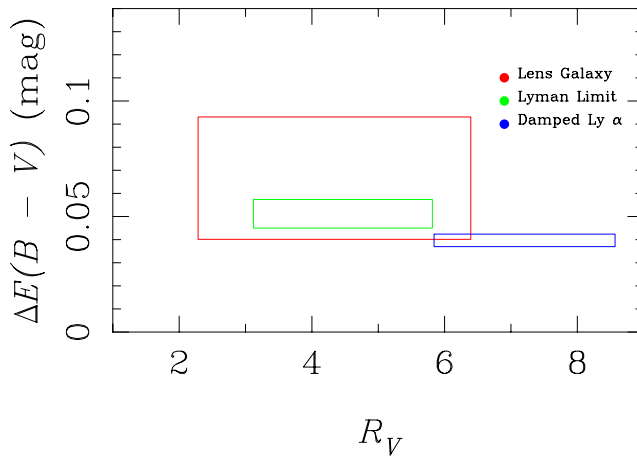


Figure 3. $\Delta E(B - V)$ and R_V for the three possible dust systems. We obtain global intervals of $\Delta E(B - V) = 0.03\text{--}0.10$ mag and $R_V = 2\text{--}9$.

photometric tasks, we infer the final global measurements. These are: $\Delta m_{AB}(\lambda_V) = 0.077 \pm 0.023$ mag and $\Delta m_{AB}(\lambda_R) = 0.022 \pm 0.013$ mag (1σ intervals), where each 1σ interval accounts for both the scatter between the typical values and the formal uncertainty of the photometric methods. The two individual contributions are added in quadrature.

4. Interpretation: extinction and microlensing

4.1. Extinction

A dust cloud in an intervening dust system may cause the relative extinction of Q0957+561A, and therefore, a chromatic increase of the magnification ratio (with respect to the radio magnification ratio). As the emission-lines do not seem to be affected by the hypothetical dust cloud, the clump of dust should be compact, i.e., it would be clearly smaller than the emission-lines regions. In Q0957+561 we have three candidates to dust system. Lens galaxies can generate differential extinction between the components of lensed quasars (Falco *et al.* 1999). Thus, the $z = 0.36$ lens galaxy is an obvious candidate. Besides the lens galaxy, there are two Ly absorption-line systems at redshifts $z = 1.1249$ and $z = 1.3911$ (e.g., Michalitsianos *et al.* 1997). The Ly object closer to the observer is a Lyman limit system. For this one, spectra of QSO 0957+561 showed that the absorption in the A component is marginally greater compared with the B component. Hence, assuming that more gas implies more dust, a relative extinction of Q0957+561A could be produced at $z = 1.1249$. On the other hand, Michalitsianos *et al.* (1997) did a detailed study of the damped Ly α system at $z = 1.3911$. In this far object, there is a strong evidence for different neutral hydrogen column densities between the lensed components, with the line of sight to image A intersecting a larger column density. This result was also claimed by Zuo *et al.* (1997), who suggested the possibility of a differential reddening by dust grains in the damped Ly α absorber.

Neglecting gravitational microlensing effects and assuming R_V -dependent Cardelli *et al.* (1989) extinction laws which are identical for both components, the dusty scenario leads to

$$\Delta m_{AB}(\lambda) = \Delta m_{AB}(\infty) + \Delta E(B - V)[a(x)R_V + b(x)] \quad (4.1)$$

where $\Delta m_{AB}(\infty)$ is the macrolens ratio or the ratio at $\lambda = \infty$ (in our case it is equal to -0.31 mag, see Introduction) and $\Delta E(B - V)$ is the differential extinction. R_V is the ratio of total to selective extinction in the V band, and $a(x)$ and $b(x)$ are known functions of $x = (1 + z_{dust})/\lambda$ (Cardelli *et al.* 1989). We take our final global measurements for the magnification ratios (see the previous section) to estimate the possible ranges of the two extinction parameters $\Delta E(B - V)$ and R_V . For a given candidate (lens galaxy, Lyman limit system or Ly α absorber), we assume that its redshift is equal to z_{dust} , and infer the possible intervals of $\Delta E(B - V)$ and R_V . In Figure 3 we show our results, so that we draw three rectangles (one for each candidate to dust system) in order to see the interval of values that we derive. The red rectangle represents the result for the lens galaxy ($z_{dust} = 0.36$), the green rectangle is the result for the Lyman limit system ($z_{dust} = 1.1249$) and the blue one corresponds to the damped Ly α system ($z_{dust} = 1.3911$). Hence, we obtain global intervals of $\Delta E(B - V) = 0.03\text{--}0.10$ mag and $R_V = 2\text{--}9$. In the Galaxy, typical paths have a ratio of total to selective extinction $R_V \approx 3.1$, while paths through typical and non-typical extinction regions have values in the range 2–6. The R_V values in far galaxies can be even higher (e.g., Falco *et al.* 1999). Therefore, most of the results on R_V seem reasonable, and only the values close to 9 may be seen as strange ones (however, see Muñoz *et al.* 2004). On the other hand, the range for differential extinction agrees with typical values in lens systems and, as a general conclusion, the observations can be

reasonably explained by means of a dusty scenario. Once again, it is important to point out that the dust cloud in the trajectory of the A beam must be compact, since the emission-lines regions do not experience differential extinction.

4.2. Microlensing

To explain the chromatic ratios, we also consider the gravitational microlensing of QSO 0957+561. While the emission-lines regions are not magnified from gravitational microlensing, the optical continuum compact sources could be affected by this physical phenomenon. We use values of the normalized surface mass density (convergence) and the shear found in Pelt *et al.* (1998) to produce 2-dimensional magnification maps with a ray shooting technique (Wambsganss 1999). With respect to the fraction of the surface mass density represented by the microlenses, we consider three cases: (a) all the mass is assumed to be in granular form (compact objects), (b) 50% of the mass in granular form, and (c) the mass is dominated by a smoothly distributed material, with only 25% of the mass in compact objects. All the microlensing objects are assumed to have a similar mass M and are distributed randomly over the lens plane. We obtain detailed results for one-solar-mass microlenses, and comment the expected results for a smaller mass. The effect of the source is taken into account by convolving a selected source intensity profile with the magnification maps. We consider two circularly-symmetric profiles: a $p = 3/2$ power-law (PL) profile and a Gaussian (GS) profile. In our model we assume that the V -band source has a characteristic length (intensity distribution) of $R_V = 3 \times 10^{14}$ cm (small source), $R_V = 10^{15}$ cm (intermediate source), or $R_V = 3 \times 10^{15}$ cm (large source), and the source size ratio $q = \frac{R_V}{R_R}$ is given by about 0.8 (standard value, see Shalyapin *et al.* 2002) or $1/3$ (arbitrary, non standard value). It is also assumed that the source, the deflector and the observer are embedded in a standard flat cosmology.

The key idea is that the VR magnification ratios are generated by two circular concentric sources with different size. The common center of the V -band and R -band sources is placed at two arbitrary pixels of the two magnification patterns (for Q0957+561A and Q0957+561B), and we look for the corresponding $[\Delta m_{AB}(\lambda_V), \Delta m_{AB}(\lambda_R)]$ pair. For a given set of physical parameters, we test a very large number of pairs of pixels (10^4) and, thus, we obtain a distribution of pairs of magnification ratios. Hence, we can compare our simulated pairs of magnification ratios with the observational ones (by plotting them in the same graph). Considering that the observational intervals contain the true ratios, we obtain an important constraint on the true pair: $d \geq 0.013$ mag, where d is the distance (in mag) from the true pair to the $\Delta m_{AB}(\lambda_V) = \Delta m_{AB}(\lambda_R)$ line in the plot. Thus, probabilities $P(d < 0.013 \text{ mag})$ are computed. When all the mass is granular and all the microlenses have one solar mass, some distributions lead to very high values of $P(d < 0.013 \text{ mag})$, so we can rule out the corresponding scenarios. On the contrary, other distributions of simulated pairs are relatively consistent with the constraint. In some cases, $P(d < 0.013 \text{ mag}) \leq 90\%$, which suggest *realistic* physical parameters, or in other words, viable scenarios. In the GS profile case, the feasible pictures are related to either the large V -band source or an intermediate V -band source together with a non-standard R -band companion. In the PL profile case, from the $P \leq 90\%$ criterion, all the scenarios seem to be plausible. When all the mass is not contained in compact objects (only the 50% or the 25%) we also compute the probabilities $P(d < 0.013 \text{ mag})$. In these cases, we infer that if the percentage of mass in compact objects decreases, it is more difficult to find scenarios in agreement with the observational constraint. We can also discuss what happens with a population of lighter microlenses, which are characterized by a mass smaller than one solar mass. Reducing the microlenses mass in a factor 100, the physical size of the magnification maps reduces in a factor 10 (the maps are 2048

pixels a side which cover a physical size of 16 Einstein radii). Then, the V -band and R -band sources with radii R_R and R_V work as the sources with radii $10 \times R_R$ and $10 \times R_V$ in the one-solar-mass case.

5. Summary and future work

We present a very robust (but no very accurate) estimation of the VR magnification ratios of QSO 0957+561. The results are consistent with two simple alternatives: a dust system between the quasar and the observer and a population of microlenses in the deflector. However, in order to decide on the true origin of both ratios (extinction, microlensing or even a mixed scenario), new observational efforts are required. For example, the GTC (a segmented 10.4 meter telescope to be installed in Canary Islands, Spain) will have an instrument (OSIRIS) with very interesting performances. OSIRIS will incorporate tunable filters with FWHM from 10^{-4} to $7 \times 10^{-3} \mu\text{m}$ over the whole optical wavelength range, and thus, tunable imaging of the two quasar components at two epochs (separated by the time delay) could lead to solve the current puzzle (dust or microlenses?) and infer tight constraints on the physical parameters of the favoured alternative. Future observations in the ultraviolet wavelength range from a space telescope may also be a decisive tool. By the way, the GLENDAMA team (<http://grupos.unican.es/glendama/>) are carrying out new studies of the system, which are based in a daily monitoring program with the 2.0m Liverpool Telescope (LT). The LT is a fully robotic telescope at the Observatorio del Roque de Los Muchachos, La Palma (Spain).

Acknowledgements

This work was supported by Instituto de Astrofísica de Canarias and Universidad de Cantabria funds, and the MCyT grants AYA2000-2111-E and AYA2001-1647-C02.

References

- Cardelli, J.A., Clayton, G.C., & Mathis, J.S. 1989, *ApJ* 345, 245.
 Conner, S.R., Lehár, J., & Burke, B.F. 1992, *ApJ* 387, L61.
 Falco, E.E., Impey, C.D., Kochanek, C.S., Lehár, J., McLeod, B.A., Rix, H.-W., Keeton, C.R., Muñoz, J.A., & Peng, C.Y. 1999, *ApJ* 523, 617.
 Michalitsianos, A.G., Dolan, J.F., Kazanas, D., Bruhweiler, F.C., Boyd, P.T., Hill, R.J., Nelson, M.J., Percival, J.W., & van Citters, G.W. 1997, *ApJ* 474, 598.
 Muñoz, J.A., Falco, E.E., Kochanek, C.S., McLeod, B.A., & Mediavilla, E. 2004, *ApJ* 605, 614.
 Ovaldsen, J.E., Teuber, J., Stabell, R., & Evans, A.K.D. 2003, *MNRAS* 345, 795.
 Pelt, J., Schild, R., Refsdal, S., & Stabell, R. 1998, *A & A* 336, 829.
 Refsdal, S., Stabell, R., Pelt, J., & Schild, R. 2000, *A & A* 360, 10.
 Schild, R.E. & Smith, R.C. 1991, *AJ* 101, 813.
 Serra-Ricart, M., Oscoz, A., Sanchís, T., Mediavilla, E., Goicoechea, L.J., Licandro, J., Alcalde, D., & Gil-Merino, R. 1999, *ApJ* 526, 40.
 Shalyapin, V.N., Goicoechea, L.J., Alcalde, D., Mediavilla, E., Muñoz, J.A., & Gil-Merino, R. 2002, *ApJ* 579, 127.
 Ullán, A., Goicoechea, L.J., Muñoz, J.A., Mediavilla, E., Serra-Ricart, M., Puga, E., Alcalde, D., Oscoz, A., & Barrena, R. 2003, *MNRAS* 346, 415.
 Wambsganss, J. 1999, *Journ. Comp. Appl. Math.* 109, 353.
 Zuo, L., Beaver, E.A., Burbidge, E.M., Cohen, R.D., Junkkarinen, V.T., & Lyons, R.W. 1997, *ApJ* 477, 568.
 Walsh, D., Carswell, R.F., & Weymann, R.J. 1979, *Nature* 279, 381.